



Universiteit
Leiden
The Netherlands

Gaining control of lipid-based nanomedicine by understanding the nano-bio interface

Pattipeiluhu, R.

Citation

Pattipeiluhu, R. (2021, December 9). *Gaining control of lipid-based nanomedicine by understanding the nano-bio interface*. Retrieved from <https://hdl.handle.net/1887/3245795>

Version: Publisher's Version

License: [Licence agreement concerning inclusion of doctoral thesis in the Institutional Repository of the University of Leiden](#)

Downloaded from: <https://hdl.handle.net/1887/3245795>

Note: To cite this publication please use the final published version (if applicable).

Chapter 4

Site Selective Binding of Apolipoprotein E in the Protein Corona of Anionic Liposomes

Protein adsorption to the surface of nanoparticles can change the *in vivo* fate of nanoparticles, for example through facilitating or inhibiting interactions with specific receptors. However, current understanding of the protein corona remains superficial, typically describing the combined effect of multiple proteins, and lacking the mechanistic understanding of individual proteins. A key challenge is deciphering the binding sites and roles of individual proteins within the protein corona of nanoparticles. Herein, we show the site-selective binding of apolipoprotein E (APOE) to anionic nanoparticles. Using a photoaffinity-based chemoproteomic approach, we were able to show the repetitive and reproducible binding of specific proteins in the protein corona of various zwitterionic and anionic liposomes and lipid nanoparticles (LNPs). Furthermore, using a competition experiment revealed that APOE binding to anionic liposomes occurs through its heparin binding domain, while APOE binding to zwitterionic liposomes and LNPs occurs in a non-heparin competitive manner through its lipid binding domain. These results greatly deepen our understanding of protein corona binding to nanoparticles towards a molecular level, and allow for the targeted design of experiments in order to determine the *in vivo* effect of single proteins in the nanoparticle protein corona.

This chapter was prepared as a research article: R. Pattipeiluhu, B.I. Florea, K. Dickie, T.H. Sharp, F. Campbell, A. Kros

4.1 Introduction

The protein corona of nanoparticles describes the preferential adsorption of proteins from a biological medium to the surface of a nanoparticle.^{1,2} Here, the alteration from a “synthetic identity” to a “biological identity” of nanoparticles is known to significantly influence the *in vivo* behavior of nanoparticles,^{3,4} for example through promotion of bodily clearance mechanisms or shielding active targeting ligands.^{5–8} Therefore, the interaction of nanoparticles with cells is, to some extent, believed to be regulated by a protein corona intermediate. The composition and complexity of the protein corona is dependent on the characteristics of the nanoparticle, such as chemical composition, size and surface charge (**Figure 1a**). Furthermore, the biological media to which the nanoparticle is exposed, as well as the kinetics of protein binding are believed to influence the protein composition.^{9,10}

These parameters have led researchers to report a large number of protein corona fingerprints, which has revealed their dynamic complexity, but also contributes to the fact that our understanding of the protein corona remains superficial and elusive, typically describing the effect of a combination of proteins, instead of more in-depth understanding of individual proteins.^{5,11,12} In addition, commonly applied methods are limited by biased isolation of large and abundant proteins, interference of endogenously present nanoparticles (*e.g.*, HDL, LDL, chylomicrons) and insufficient or non-native isolation of nanoparticle-protein complexes.^{13–15} The resulting protein corona fingerprints generated are therefore typically long and empirical lists, displaying high similarity despite large differences in the synthetic identity of the nanoparticles.^{7,16–18} Furthermore, the majority of these methods do not allow validation of binding for the discovered hits, hindering the confirmation and in-depth understanding of key nanoparticle-protein interactions. Recently, more research has been dedicated towards the development of new methods for the identification and validation of the protein corona on nanoparticles.^{19,20} We have, to this end, developed a bifunctional lipid probe (IKSo2, **Figure 1b**) for a photoaffinity-based chemoproteomic approach in order to covalently capture, isolate and identify the protein corona on liposomes in human plasma (**Figure 1c**).²¹ Utilizing the covalent capture of adsorbed proteins allowed us to validate the selectivity of protein binding *in vitro*, crucially complementing the initial hit from a complex biological system.

Here, we employ this photoaffinity based chemoproteomics method for the identification of the protein corona on ionizable lipid nanoparticles (LNPs) encapsulating siRNA, which highly complements key nanoparticle-protein interactions described in literature. Furthermore, we are able to compare these findings to liposome formulations with distinct synthetic identities, and consequently pinpoint reproducible and selective binding of

individual proteins. Specifically, we show that apolipoprotein E (APOE) binds to a variety of anionic liposomes, but only a subset of zwitterionic neutral lipidic nanoparticles. Using a competition assay, we reveal that this APOE binding to anionic liposomes occurs site selectively through its heparin binding domain. Our findings display a unique selectivity of an individual protein in the protein corona of various nanoparticles, which contributes to the deeper understanding of nano-bio interactions and will allow for the specific mechanistic evaluation of these nanoparticles *in vivo*.

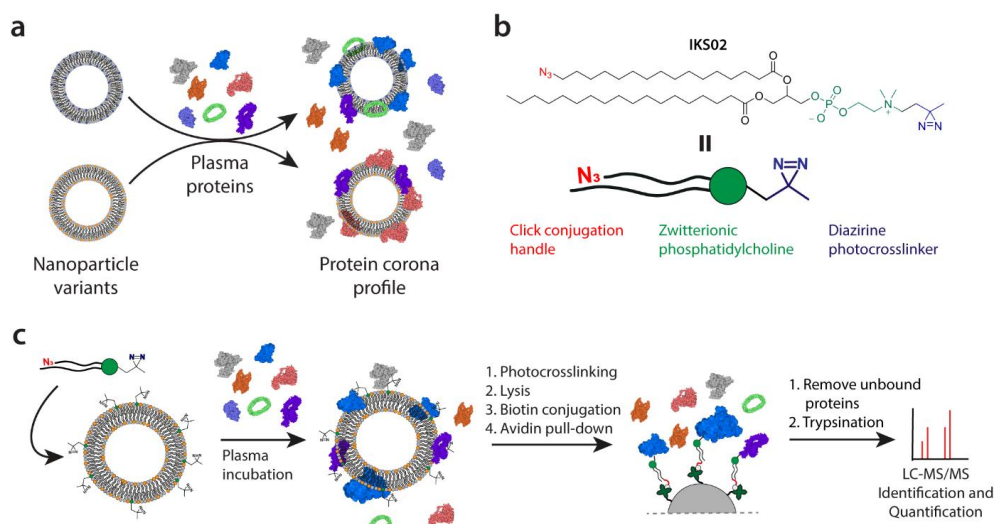


Figure 1. Photoaffinity based chemoproteomic approach for the identification of the liposome protein corona. (a) Schematic representation of how nanoparticle variation can lead to alteration of the protein corona profile. (b) Structure and schematic of bifunctional lipid probe IKSo₂, containing a diazirine photo crosslinker, zwitterionic phosphatidylcholine and azide functionality for click chemistry conjugation. (c) Methodology for identification of the liposome protein corona by co-formulation with IKSo₂, followed by incubation, crosslinking, pull-down and LC-MS/MS identification and quantification. Protein structures were obtained from the protein data bank (PDB) and their depiction was generated using Illustrate.²²

4.2 Results

Our first goal was aimed at expanding the photoaffinity-based chemoproteomic approach for the identification of the protein corona of LNPs. LNPs are multicomponent systems typically consisting of an ionizable lipid (*e.g.*, DLin-MC₃-DMA),²³ structural lipid (*e.g.*, cholesterol), helper lipid (*e.g.*, DSPC), PEG lipid and an oligonucleotide payload (*e.g.*, mRNA, siRNA).^{24,25} LNPs have realized the transition of RNA therapeutics to the clinic,

serving as state-of-the-art carriers for the cytosolic delivery of RNA molecules. In 2018, Onpatro® was approved as the first RNA interference (RNAi) drug, used for the treatment of hereditary ATTR amyloidosis by delivering siRNA molecules to liver hepatocytes.²⁶ More recently, LNPs have been utilized for the delivery of mRNA for the safe and efficient development of prophylactic vaccines against SARS-CoV-2.^{27,28} Currently, there is a large variety of LNP formulations being studied, composed of typically novel or proprietary ionizable lipids (ILs).²⁹

In our approach, we studied the Onpatro® formulation, with its siRNA cargo Patisiran®,³⁰ for two distinct reasons. Firstly, the organization of lipids within this formulation has been studied in-depth, showing that the surface of this nanoparticle is enriched with 1,2-distearoyl-sn-glycero-3-phosphocholine (DSPC) and 1,2-Dimyristoyl-*rac*-glycero-3-methoxypolyethylene glycol-2000 (DMG-PEG2000) (**Figure 2a**).³¹ In addition, it has been shown that exchanging DSPC in this formulation with similar analogues keeps this surface enrichment intact.³² With IKS02 being a close mimic of DSPC, we hypothesized that this lipid would be sufficiently enriched at the surface of these LNPs in order to enable crosslinking of the protein corona. Secondly, the importance of APOE is known in relation to its *in vivo* effect, where its presence in plasma is required for the efficient uptake of LNPs and silencing the target protein in liver hepatocytes through the lipoprotein-receptor family.^{33,34} Together, these findings suggest a crucial role for the binding of APOE to the LNP surface and thereby serves as a fitting positive control for our identification method. To this end, we incorporated IKS02 at 5 mol%, exchanging for DSPC, and performed the assembly using conventional microfluidic procedures. Cryogenic transmission electron microscopy (cryoTEM), dynamic light scattering (DLS) and ζ -potential measurements of LNPs formulated with IKS02, compared to the native Onpatro® formulation, revealed no significant changes in nanoparticle morphology, size and surface charge (**Figure 2b,c and Table S1**). Following assembly, LNPs were incubated in full human plasma for 1 hour at 37 °C, followed by crosslinking with UV-A light (350 nm, 15 min) to capture the adsorbed proteins. The mixture was lysed, the proteins were precipitated and biotin was conjugated to the crosslinked lipid-protein conjugates through copper-catalyzed click chemistry, followed by pull-down using avidin-agarose beads. Finally, on-bead digestion allowed for the LC-MS/MS identification and quantification of the proteins. In order to correctly identify hits from this method, a negative control in which the sample is not irradiated with UV-A light was employed, allowing for a comparison to the background labeling observed due to the copper catalyzed click chemistry. The quantified proteins are displayed in a volcano plot describing the abundance (>1.5-fold) and statistical significance ($p < 0.05$) of proteins in the “+UV” sample over the “-UV” control (**Figure 2d**). Proteins meeting these

criteria are selected as hits and can be sorted based on relative abundance derived from their label free quantification within the sample (**Figure 2e**). From these results, APOE is positively identified at a relative abundance of ~25%. Furthermore, the protein corona of Onpattro® is dominated by other apolipoproteins, such as APOA1 and apoB. These findings highlight the large similarity of this LNP formulation to endogenous nanoparticles such as low-density lipoprotein (LDL), and support the fact that this LNPs exploits similar endogenous uptake mechanisms through a protein corona intermediate.

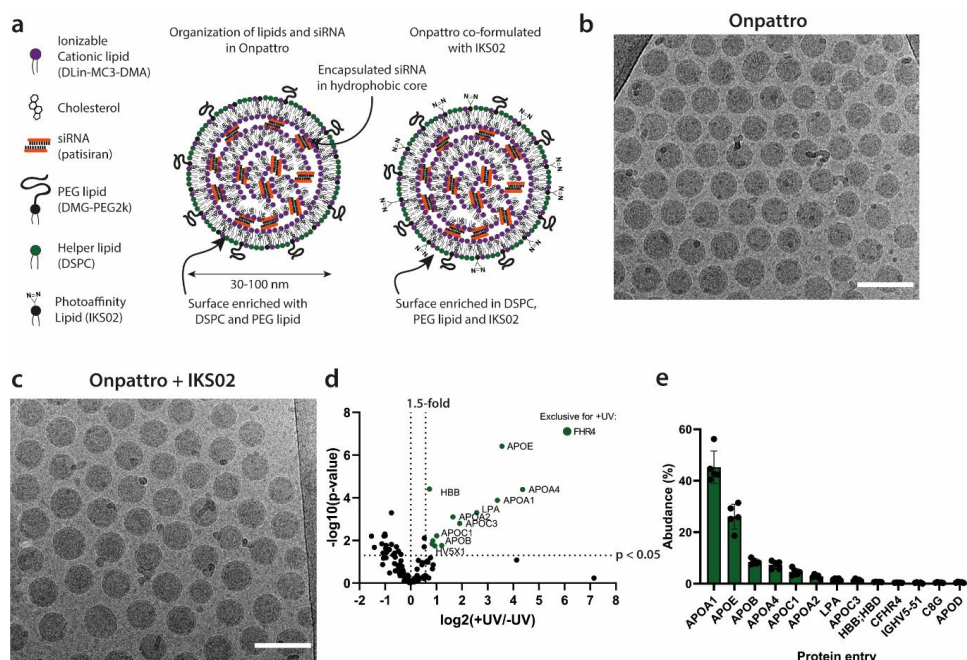


Figure 2. Application of photoaffinity based chemoproteomic approach for the identification of the protein corona of LNPs. (a) Schematic representation of the lipid organization in LNPs. Surface enriched DSPC can be replaced by IKS02. (b,c) CryoTEM images of native Onpattro and Onpattro co-formulated with 5 mol% of IKS02. Scale bars are 100 nm. (d) Volcano plot of identified proteins of “+UV” and “-UV”. Hits were selected when meeting the criteria for p -values ($p < 0.05$) and enrichment (>1.5 -fold) and are displayed in green. (e) Protein abundance of identified hits described in d. Bar plots and errors bars represent the average ($n = 5$) and standard deviation.

Previously, we have reported the protein corona of anionic liposomes, with the lipid composition of Ambisome®,^{35,36} where APOE was found as the most abundant protein of its protein corona.²¹ The high abundancy of a single protein on two very distinct lipid surfaces, anionic Ambisome® vs. zwitterionic neutral Onpattro®, raises the question to

what extent APOE binding is determined by surface charge. Although liposomes and LNPs both have solvent-exposed lipidic surfaces, they differ significantly in their structural organization. Liposomes are unilamellar vesicles with an aqueous core in which a bilayer structure is exposed to the exterior. LNPs, however, are solid core structures that contain a lipid monolayer enriched with PEGylated lipids on their surface (**Figure 2a**). Since the assembly of liposomes with distinct physiochemical properties (*e.g.*, size, rigidity, surface charge) can be achieved with a higher degree of precision and flexibility over LNPs, we assessed multiple liposomal formulations in order to probe the repetitive binding of APOE and other proteins in their protein corona (**Figure 3a**).

Firstly, we selected a liposomal formulation with a similar behavior to Onpattro®, serving as a positive control of liposomes exhibiting an APOE dependent uptake mechanism. Liposomes composed of zwitterionic neutral 1,2-distearoyl-*sn*-glycero-3-phosphocholine (DSPC, 60 mol%) and cholesterol (40 mol%) were reported to have a >20-fold reduced uptake into liver hepatocytes in APOE-deficient mice,³⁷ highlighting the importance of APOE binding for its *in vivo* fate. Secondly, we selected an anionic liposome formulation based on the lipid composition of Mepact® (30PS), composed of anionic 1,2-dioleoyl-*sn*-glycero-3-phospho-L-serine (DOPS, 30 mol%) and zwitterionic lipid 1-palmitoyl-2-oleoyl-glycero-3-phosphocholine (POPC, 70 mol%), used with its active ingredient Mifamurtide in the clinic for the treatment of high-grade resectable non-metastatic osteosarcoma.³⁸ As controls of anionic lipid type and surface charge, we also included liposomal formulations where DOPS was replaced with the anionic lipid 1,2-dioleoyl-*sn*-glycero-3-phospho-(1'-rac-glycerol) (DOPG, 30PG) or the zwitterionic lipid 1,2-dioleoyl-*sn*-glycero-3-phosphocholine (DOPC, 30PC) (**Figure 3b**). Furthermore, we systematically varied the ratio of anionic and zwitterionic lipid in these formulations to determine to what extent surface charge density would affect protein binding (**Figure 3a**, 10PS, 95PS, 10PG, 50PG, 70PG, 95PG, 95PC). All liposomal formulations contained 5 mol% of the photoaffinity probe IKS02 and were assembled using standard thin film hydration and extrusion protocols, yielding monodisperse liposomes with an average size of ~100 nm (PDI < 0.120) (**Table S1**). All formulations were processed through our photoaffinity based chemoproteomic workflow and the criteria for the positive identification of protein hits from their respective volcano plots was equal to those applied for the determination of the Onpattro® protein corona (**Figures S1-4**). From the combination of these identified hits, we constructed a heatmap displaying the relative abundance of all proteins within their respective protein corona (**Figure S5**). Overall, the obtained protein coronas of these liposomal formulations are generally dominated by the identification of apolipoproteins (**Figure 3c**).

When comparing the anionic liposomes, a more negative ζ -potential for PG liposomes (10PG, 30PG, 50PG, 70PG, 95PG), led to a clear increase in total number of proteins in the protein corona, albeit at an increased amount of identified proteins at low abundance (< 2%) (**Figure 3d, Figure S5**). Nevertheless, for 30PS and 95PS, which showed similar strongly anionic surface potentials, no significant increase in number of proteins in their respective corona was observed (**Figure 3d, Figure S5**). These results indicate that protein corona complexity on anionic liposomes is not only dependent on the surface charge density, but also on lipid headgroup structure.

The rather sparse protein corona obtained for PS-containing liposomes, compared to PG-containing liposomes, may be a consequence of the biological role of PS, which must remain exposed. In nature, PS lipids are commonly present in negatively-charged biological membranes, predominantly in the inner leaflet or the subcellular compartments of healthy cells, where they function as signaling molecules for downstream processes.^{39,40} However, PS lipids can be exposed extracellularly by the help of lipid scramblases during biological processes such as apoptosis.^{41,42} In vivo, PS lipids must be directly engaged by specific receptors of phagocytic cells (*e.g.* macrophages) to mediate recognition, without being masked by proteins bound to the exposed PS.^{42,43} Furthermore, the absence of a dense or complex protein corona supports the *in vivo* recognition and selective uptake by macrophages and other phagocytic cells which is reported for the Mepact® formulation.^{38,44,45}

For the weakly anionic (10PS, 10PG) and zwitterionic liposomes (DSPC-Chol, 30PC, 95PC), the number of bound proteins varied widely. For example, 10PG was completely devoid of positive protein identification, whereas APOA1 was the only identified hit in the case of 10PS. Furthermore, zwitterionic 30PC also shows a low amount of protein binding and is similar to our previous protein corona determined on POPC-Cholesterol (50 mol% POPC, 45% mol% cholesterol, 5 mol% IKS02).²¹ Nevertheless, 95PC and DSPC-Chol showed an increase in total numbers of protein binding. Although the antifouling behavior of zwitterionic neutral nanoparticles and surfaces is a frequently described phenomenon,⁴⁶⁻⁴⁸ in the case of zwitterionic liposomes other membrane characteristics such as rigidity or solvent exposed hydrophobicity might also play a role in the binding affinity towards plasma proteins.

From the identified apolipoproteins across all formulations, it is apparent that apolipoprotein A-1 (APOA1) and APOE showed the most repetitive and reproducible binding. In the case of DSPC-Chol, we positively identified the binding of APOE, as expected due to its importance in *in vivo* fate of these liposomes.³⁷ Nevertheless, the APOE

binding was not observed for the other zwitterionic liposomes. In the case of anionic liposomes, positive APOE binding was observed across all strongly anionic formulations irrespective of headgroup structure (PS or PG), but not for weakly anionic liposomes (10PS, 10PG). This indicates that the binding of APOE to anionic liposomes has a certain threshold requirement for surface charge density.

In the case of APOA1, positive binding is observed for all formulations besides DSPC-Chol, 30PC and 10PG. APOA1 is a 28 kDa protein and a major component of high-density lipoproteins (HDL), where it plays important roles in promoting cellular cholesterol efflux, binding lipids, activating lecithin cholesterol acyltransferase, and aiding in the structural stability of mature HDL that interacts with specific receptors and lipid transfer proteins.⁴⁹ APOA1 is known to interact with zwitterionic and anionic lipid surfaces through both headgroup and hydrophobic interactions, due to the multiple structural conformations it can adopt.^{50–52} Its primary identified lipid bound structure consists of pseudo-continuous amphipathic α -helices, forming a toroidal structure (**Figure S6**, PDB: 1AV1).⁵³ APOA1 has hydrophobic patches and a large amount of charged residues across its surface to facilitate the binding to lipidic surfaces. However, APOA1 does not have specific binding domains for other biomolecules. The high affinity of APOA1 towards lipid surfaces, both anionic and zwitterionic, explains the high abundance of this protein in the protein corona of multiple liposomal formulations. However, the large number interaction possibilities of APOA1 with lipid surfaces makes it difficult to determine why APOA1 is absent in the protein corona of certain liposomes.

APOE is a 36 kDa glycoprotein and associated with nearly all lipoproteins in human plasma (*e.g.*, LDL, HDL, Chylomicrons).^{54,55} One of the key functions of APOE is mediating the binding of lipoproteins in plasma to specific cell-surface receptors (*e.g.*, LDLr, LRP), allowing the internalization of APOE-containing lipoprotein particles. In order to exhibit this role, APOE has an amphipathic α -helical C-terminal domain critical for the binding to lipoproteins (**Figure 3e**).^{56,57} Binding of lipoproteins promotes a structural change, facilitated through a flexible hinge domain, to the putative “open state” of APOE (**Figure 3e**). This lipidated and open state of APOE exposes a LDLr-binding region,^{58,59} containing a heparan sulfate proteoglycan (HSPG) recognition sequence.⁶⁰ The recognition of cell-surface HSPGs is required for the binding and uptake of APOE-containing lipoproteins by transfer to lipoprotein receptors or through HSPG directly.^{61–63} Furthermore, an additional heparin binding-site is present on the “closed state” of APOE, containing a variety of lysine (Lys-143, Lys-146 and Lys-233) and arginine (Arg-142, Arg-145, and Arg-147) residues.^{64,65} In this binding-site, Lys-233 is critical for effective heparin binding in the closed state, but also

overlaps with the C-terminal lipid binding region. Here, we hypothesized that APOE binding to anionic liposomes might occur through this surface exposed heparin binding domain.

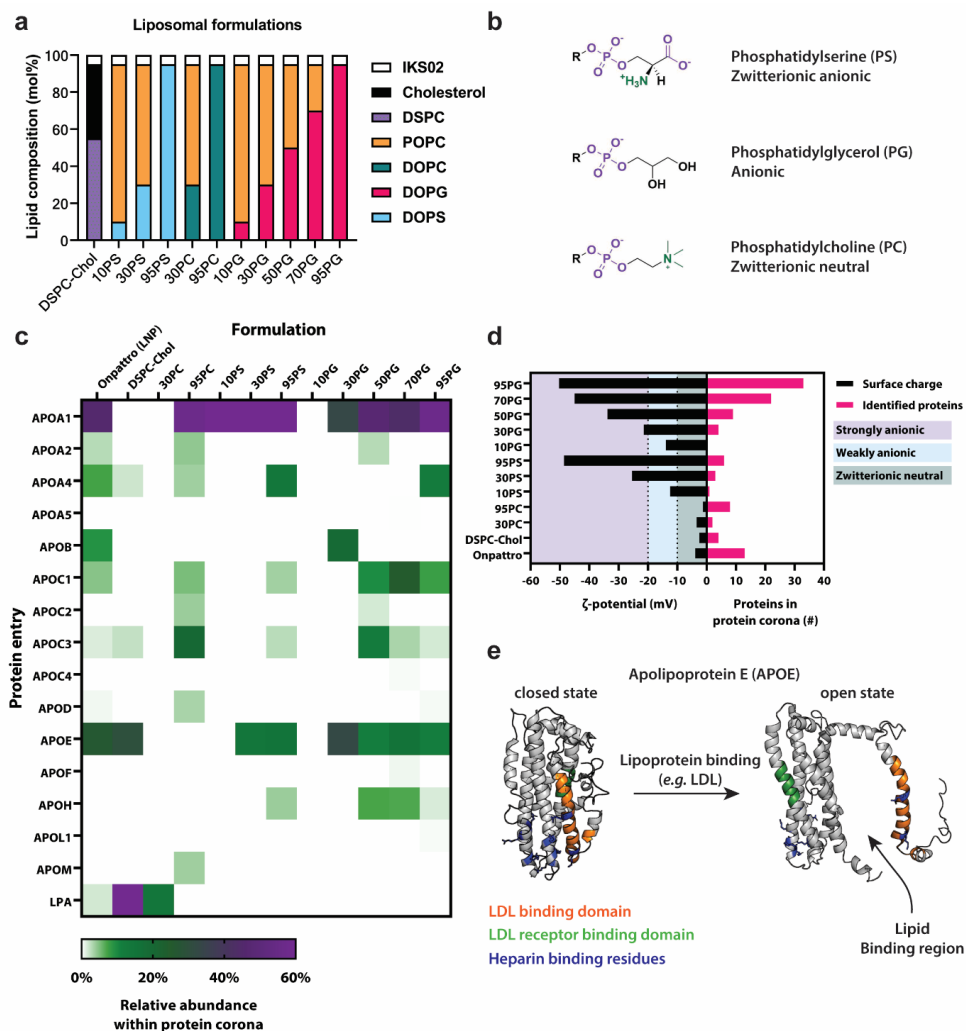


Figure 3. Protein corona identification of zwitterionic and anionic liposomes. (a) Lipid type and composition of liposomal formulations in the screen of protein corona fingerprints. (b) Chemical structures of anionic and zwitterionic lipid headgroups. Moieties responsible for anionic charge displayed in purple and for cationic charge in green. (c) Heatmap displaying the LFQ abundance of the identified protein corona of all liposomal formulations and Onpatro®. The abundance is displayed as relative to other proteins within the protein corona. (d) Surface charge (ζ -potential)

and number of identified proteins in the protein corona of all liposomal formulations and Onpattro®. (e) Different structural conformations of APOE and important binding domains and residues. Cationic residues on the surface indicated in blue make up the heparin binding domain.⁶⁴ Interaction of the LDL binding domain (orange) upon binding to lipoproteins leads to the reorganization of the protein into an “open state” which exposes the LDL receptor binding domain critical for cellular uptake.⁶⁶ PDB entry 2L7B is used for APOE closed state,⁶⁵ the open state has been generated using PyMOL.

In order to validate the binding specificity of APOE and APOA1 to liposomes and LNPs, and the possible role of specific domains on liposome binding, we performed a competition assay using a mixture of purified human proteins and potential competitors (**Figure 4a**). The protein mixture was composed of APOE and APOA1, and complemented with abundant plasma proteins that were not identified as positive hits in their protein coronas; specifically prothrombin (THRB), transferrin (TRFE) and albumin (ALBU). Within this mixture, the ratio of proteins was chosen to reflect their natural abundance in plasma.⁶⁷ In this assay, liposomes or LNPs of interest containing IKS02 were added to the mixture, followed by the addition of a competitor, and incubated at 37 °C for 1 hour. After irradiation and click chemistry conjugation with a fluorescent dye (Cy5-alkyne), the binding of proteins and potential inhibition by the competitors was determined by in-gel fluorescence (**Figure 4a**). In the case of anionic liposome formulations, 30PS and 30PG were selected and showed very similar competitive binding to APOE. In these cases, the binding of APOE and APOA1 was validated by its presence in the “+UV” lane and absence in “-UV”, while the other proteins remained at background levels in both cases (**Figure 4b,c**). Competition with heparin (5:1 heparin:APOE, mol:mol) was enough to completely abolish the binding of APOE to both of these liposomes. Moreover, this competitive binding led to an increase in APOA1 signal, confirming that APOA1 does not bind anionic liposomes through any form of heparin binding domain. Furthermore, competition with native DSPC-Chol or 30PC liposomes did not affect APOE or APOA1 binding to these anionic liposomes.

In the case of zwitterionic 30PC, we did not observe any positive labeling of proteins, confirming the lack of binding affinity of all selected proteins to these liposomes, in agreement with our initial experiment in human plasma (**Figure 4d**). In the case of DSPC-Chol and Onpattro®, the validation was also in line with our initial screen, showing a positive binding of APOE in both cases, but a lack of APOA1 binding in the case of DSPC-Chol (**Figure 4e,f**). For these formulations, the competition with heparin showed no decrease in APOE binding. However, the addition of 30PG did lead to competition for APOE binding in the case of DSPC-Chol. This indicates that APOE binding to anionic liposomes through its heparin binding domain has a higher affinity than through its lipid

binding region, likely due to stronger electrostatic interactions of the surface exposed cationic residues with the anionic lipids compared to hydrophobic driven interaction of the lipid binding region. Altogether, the high degree of competition between heparin and anionic liposomes shows that APOE binds to anionic liposomes through its surface exposed heparin binding domain. Given the critical importance of residue Lys-233 in heparin binding, which overlaps with the C-terminal lipid binding domain,^{63,64} this would likely lead to a “locked closed state” of APOE due to the strong electrostatic interaction with all the residues (**Figure 4g**). The binding of APOE to spherical zwitterionic lipoproteins surfaces is known to occur in a multi-step reversible process in which the hydrophobic interaction of the lipid binding domain and flexible hinge regions facilitate a structural change.^{66,68} Therefore, we assume that APOE binding to DSPC-Chol and Onpattro® occurs through its lipid binding region, similar to the binding to zwitterionic lipoproteins, resulting in a non-competitive binding with heparin (**Figure 4g**).

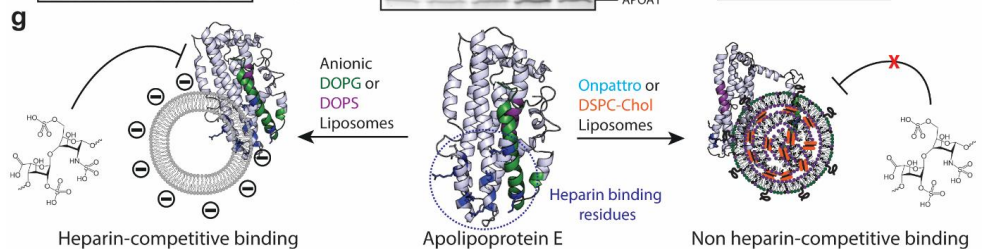
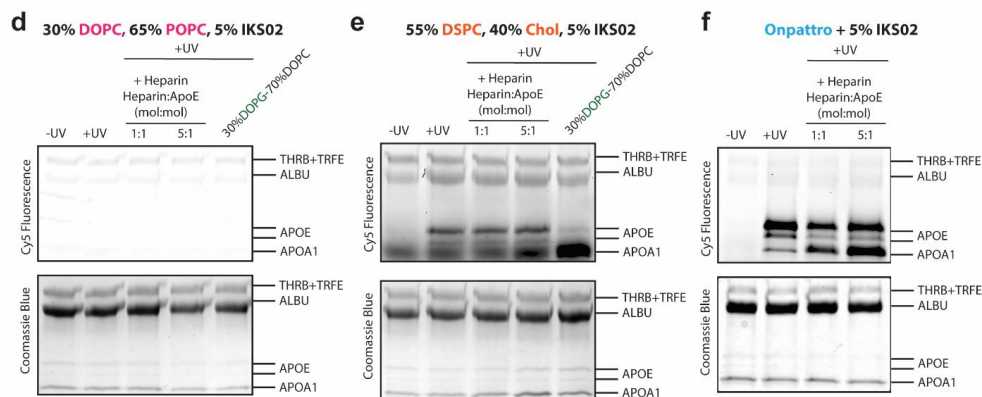
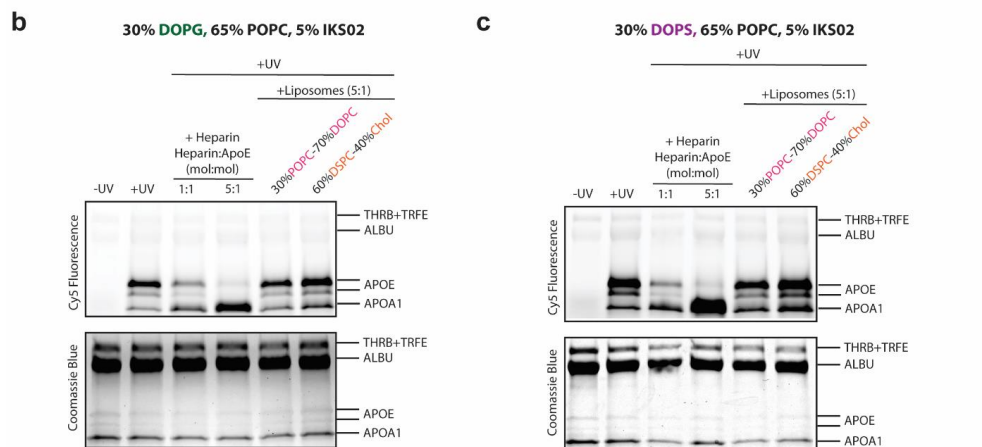
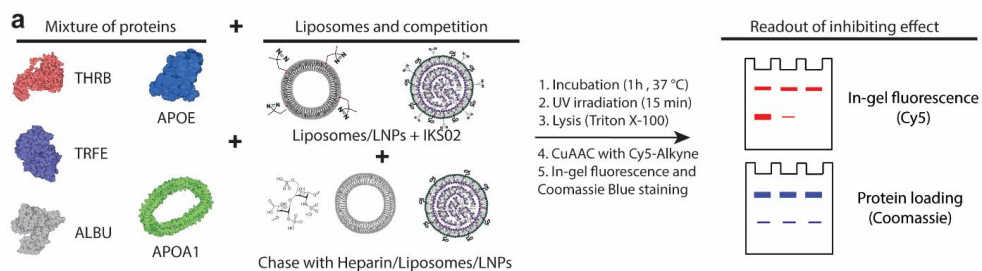


Figure 4. Site selective binding of APOE to anionic liposomes. (a) Schematic representation of the employed competition assay. Protein structures were obtained from the PDB (entries: THRB = 6C2W⁶⁹, TRFE = 1D3K⁷⁰, ALBU = 1E78⁷¹, APOA1 = 1AV1⁵³, APOE = 2L7B⁶⁵) and illustrations were generated using Illustrate.²² (b-f) In-gel fluorescence (Cy5) and Coomassie Blue stained SDS-PAGE gels of competition experiments. APOE appears as two distinct bands on SDS-PAGE, due to the presence of its glycosylated (36 kDa) and non-glycosylated (34 kDa) form.⁷² (g) Schematic representation of the competitive binding of heparin to anionic liposomes 3oPG and 3oPS, and the lack thereof in the case of DSPC-Chol and Onpattro. Heparin binding residues are displayed in blue. Lipid binding region is displayed in green. LDLr binding is displayed in purple.

4.3 Discussion

Using a photoaffinity-based chemoproteomics approach, we have identified and validated the recurring binding of various proteins on liposomes and LNPs. In particular, we have been able to validate the positive binding of APOE on Onpattro® LNPs and DSPC-Chol liposomes, for which their importance has been described in literature. Furthermore, we have shown to what extent APOE binding is repetitive among zwitterionic and anionic liposomes. Finally, we were able to use the photoaffinity approach in combination with a competition assay in order to determine that APOE binds strongly-anionic liposomes through its heparin binding domain. In addition, binding to zwitterionic liposomes and LNPs occurs non-competitively with heparin, likely in a similar manner as APOE binding and structural reorganization to spherical lipoproteins.

While the current understanding of the protein corona is known at a superficial level, typically describing the effect of a set of proteins, with these results we have gained important insights into specific protein-nanoparticle interactions. Understanding site-selective binding of a single protein to LNPs in plasma will allow us to probe the effect on its fate *in vivo*. While the effect of APOE in the uptake of liver hepatocytes has been shown for zwitterionic liposomes such as DSPC-Chol,³⁷ of particular interest is understanding to which extent binding of APOE to anionic liposomes has on its uptake *in vivo*. Previous work has shown that anionic nanoparticles are preferentially taken up through scavenger receptors (*e.g.*, stabilin-1,2) preferentially expressed by cells of the reticuloendothelial system (RES).^{32,73,74} However, the intermediate function of APOE is not understood. In future work, we aim to compare the biodistribution of anionic and zwitterionic liposomes in wildtype and APOE knockout (*apoE*^{-/-}) mice in order to examine the role of APOE on the uptake by liver cells.

With the current widespread application of multiple LNP-based therapeutics, such as the nascent prophylactic vaccines against SARS-CoV-2, we believe that this system can be used

for screening protein coronas on other LNP formulations. The ability to validate specific protein binding, and gain more insight into their relevant binding domains and resulting cell uptake pathways will aid our understanding of the nano-bio interface at a much deeper level, improving the *in vivo* fate prediction of LNPs and liposomal formulations.

4.4 References

1. Cai, R. & Chen, C. The Crown and the Scepter: Roles of the Protein Corona in Nanomedicine. *Adv. Mater.* **1805740**, 1–13 (2018).
2. Walkey, C. D. & Chan, W. C. W. Understanding and controlling the interaction of nanomaterials with proteins in a physiological environment. *Chem. Soc. Rev.* **41**, 2780–2799 (2012).
3. Lundqvist, M. *et al.* The nanoparticle protein corona formed in human blood or human blood fractions. *PLoS One* **12**, 1–15 (2017).
4. Monopoli, M. P., Aberg, C., Salvati, A. & Dawson, K. A. Biomolecular coronas provide the biological identity of nanosized materials. *Nat. Nanotechnol.* **7**, 779–786 (2012).
5. Salvati, A. *et al.* Transferrin-functionalized nanoparticles lose their targeting capabilities when a biomolecule corona adsorbs on the surface. *Nat. Nanotechnol.* **8**, 137–143 (2013).
6. Bertrand, N. *et al.* Mechanistic understanding of *in vivo* protein corona formation on polymeric nanoparticles and impact on pharmacokinetics. *Nat. Commun.* **8**, 777 (2017).
7. Gunawan, C., Lim, M., Marquis, C. P. & Amal, R. Nanoparticle–protein corona complexes govern the biological fates and functions of nanoparticles. *J. Mater. Chem. B* **2**, 2060–2083 (2014).
8. Chinen, A. B., Guan, C. M., Ko, C. H. & Mirkin, C. A. The Impact of Protein Corona Formation on the Macrophage Cellular Uptake and Biodistribution of Spherical Nucleic Acids. *Small* **13**, 1603847 (2017).
9. Vilanova, O. *et al.* Understanding the Kinetics of Protein-Nanoparticle Corona Formation. *ACS Nano* **10**, 10842–10850 (2016).
10. Casals, E., Pfaller, T., Duschl, A., Oostingh, G. J. & Puentes, V. Time evolution of the nanoparticle protein corona. *ACS Nano* **4**, 3623–3632 (2010).
11. Oh, J. Y. *et al.* Cloaking nanoparticles with protein corona shield for targeted drug delivery. *Nat. Commun.* **9**, 1–9 (2018).
12. Tenzer, S. *et al.* Rapid formation of plasma protein corona critically affects nanoparticle pathophysiology. *Nat. Nanotechnol.* **8**, 772 (2013).
13. Weber, C., Morsbach, S. & Landfester, K. Possibilities and Limitations of Different Separation Techniques for the Analysis of the Protein Corona. *Angew. Chemie Int. Ed.* **58**, 12787–12794 (2019).
14. Simonsen, J. B. & Münter, R. Pay attention to the biological nanoparticles when studying the protein corona on nanomedicines. *Angew. Chemie Int. Ed.* **59**, 12584–12588 (2020).
15. Kristensen, K. *et al.* Isolation methods commonly used to study the liposomal protein corona suffer from contamination issues. *Acta Biomater.* **65**, In press (2021).
16. Pozzi, D. *et al.* The biomolecular corona of nanoparticles in circulating biological media. *Nanoscale* **7**, 13958–13966 (2015).
17. Bigdeli, A. *et al.* Exploring Cellular Interactions of Liposomes Using Protein Corona Fingerprints and Physicochemical Properties. *ACS Nano* **10**, 3723–3737 (2016).
18. Walkey, C. D. *et al.* Protein Corona Fingerprinting Predicts the Cellular Interaction of Gold

- and Silver Nanoparticles. *ACS Nano* **8**, 2439–2455 (2014).
19. Zhang, Y., Wu, J. L. Y., Lazarovits, J. & Chan, W. C. W. An Analysis of the Binding Function and Structural Organization of the Protein Corona. *J. Am. Chem. Soc.* **142**, 8827–8836 (2020).
 20. Chu, Y. *et al.* Deciphering Protein Corona by scFv-Based Affinity Chromatography. *Nano Lett.* **21**, 2124–2131 (2021).
 21. Pattipeiluhu, R. *et al.* Unbiased Identification of the Liposome Protein Corona using Photoaffinity-based Chemoproteomics. *ACS Cent. Sci.* **6**, 535–545 (2020).
 22. Goodsell, D. S., Autin, L. & Olson, A. J. Illustrate: Software for Biomolecular Illustration. *Structure* **27**, 1716–1720 (2019).
 23. Jayaraman, M. *et al.* Maximizing the potency of siRNA lipid nanoparticles for hepatic gene silencing in vivo. *Angew. Chemie - Int. Ed.* **51**, 8529–8533 (2012).
 24. Cullis, P. R. & Hope, M. J. Lipid Nanoparticle Systems for Enabling Gene Therapies. *Mol. Ther.* **25**, 1467–1475 (2017).
 25. Witzigmann, D. *et al.* Lipid nanoparticle technology for therapeutic gene regulation in the liver. *Adv. Drug Deliv. Rev.* **159**, 344–363 (2020).
 26. Akinc, A. *et al.* The Onpattro story and the clinical translation of nanomedicines containing nucleic acid-based drugs. *Nat. Nanotechnol.* **14**, 1084–1087 (2019).
 27. Jackson, L. A. *et al.* An mRNA Vaccine against SARS-CoV-2 — Preliminary Report. *N. Engl. J. Med.* **383**, 1920–1931 (2020).
 28. Zhang, N.-N. *et al.* A Thermostable mRNA Vaccine against COVID-19. *Cell* **182**, 1271–1283 (2020).
 29. Rietwyk, S. & Peer, D. Next-Generation Lipids in RNA Interference Therapeutics. **11**, 7572–7586 (2017).
 30. Adams, D. *et al.* Patisiran, an RNAi therapeutic, for hereditary transthyretin amyloidosis. *N. Engl. J. Med.* **379**, 11–21 (2018).
 31. Arteta, M. Y. *et al.* Successful reprogramming of cellular protein production through mRNA delivered by functionalized lipid nanoparticles. *Proc. Natl. Acad. Sci. U. S. A.* **115**, E3351–E3360 (2018).
 32. Pattipeiluhu, R. *et al.* Anionic Lipid Nanoparticles Preferentially Deliver mRNA to the Hepatic Reticuloendothelial System. *Chapter 3, This Thesis* (2021).
 33. Akinc, A. *et al.* Targeted delivery of RNAi therapeutics with endogenous and exogenous ligand-based mechanisms. *Mol. Ther.* **18**, 1357–1364 (2010).
 34. Sabnis, S. *et al.* A Novel Amino Lipid Series for mRNA Delivery: Improved Endosomal Escape and Sustained Pharmacology and Safety in Non-human Primates. *Mol. Ther.* **26**, 1509–1519 (2018).
 35. Bekersky, I. *et al.* Pharmacokinetics, excretion, and mass balance of liposomal amphotericin B (AmBisome) and amphotericin B deoxycholate in humans. *Antimicrob. Agents Chemother.* **46**, 828–833 (2002).
 36. Bulbake, U., Doppalapudi, S., Kommineni, N. & Khan, W. Liposomal Formulations in Clinical Use: An Updated Review. *Pharmaceutics* **9**, 12 (2017).
 37. Yan, X. *et al.* The role of apolipoprotein E in the elimination of liposomes from blood by hepatocytes in the mouse. *Biochem. Biophys. Res. Commun.* **328**, 57–62 (2005).
 38. Fidler, I. J., Sone, S., Fogler, W. E. & Barnes, Z. L. Eradication of spontaneous metastases and activation of alveolar macrophages by intravenous injection of liposomes containing muramyl dipeptide. *Proc. Natl. Acad. Sci.* **78**, 1680–1684 (1981).
 39. Yeung, T. *et al.* Membrane Phosphatidylserine Regulates Surface Charge and Protein Localization. *Science* **319**, 210–213 (2008).

40. Arumugam, S. & Kaur, A. The Lipids of the Early Endosomes: Making Multimodality Work. *Chembiochem* **18**, 1053–1060 (2017).
41. Hanayama, R. *et al.* Autoimmune Disease and Impaired Uptake of Apoptotic Cells in MFG-E8-Deficient Mice. *Science* **304**, 1147–1150 (2004).
42. Allen, T. M., Williamson, P. & Schlegel, R. A. Phosphatidylserine as a determinant of reticuloendothelial recognition of liposome models of the erythrocyte surface. *Proc. Natl. Acad. Sci.* **85**, 8067–8071 (1988).
43. Lemke, G. How macrophages deal with death. *Nat. Rev. Immunol.* **19**, 539–549 (2019).
44. Ando, K., Mori, K., Corradini, N., Redini, F. & Heymann, D. Mifamurtide for the treatment of nonmetastatic osteosarcoma. *Expert Opin. Pharmacother.* **12**, 285–292 (2011).
45. Mori, K., Ando, K. & Heymann, D. Liposomal muramyl tripeptide phosphatidyl ethanolamine: a safe and effective agent against osteosarcoma pulmonary metastases. *Expert Rev. Anticancer Ther.* **8**, 151–159 (2008).
46. Debayle, M. *et al.* Zwitterionic polymer ligands: an ideal surface coating to totally suppress protein-nanoparticle corona formation? *Biomaterials* **219**, 119357 (2019).
47. Safavi-Sohi, R. *et al.* Bypassing Protein Corona Issue on Active Targeting: Zwitterionic Coatings Dictate Specific Interactions of Targeting Moieties and Cell Receptors. *ACS Appl. Mater. Interfaces* **8**, 22808–22818 (2016).
48. Sanchez-Cano, C. & Carril, M. Recent Developments in the Design of Non-Biofouling Coatings for Nanoparticles and Surfaces. *International Journal of Molecular Sciences* **21**, 1007 (2020).
49. Frank, P. G. & Marcel, Y. L. Apolipoprotein A-I: structure-function relationships. *J. Lipid Res.* **41**, 853–872 (2000).
50. Sparks, D. L., Lund-Katz, S. & Phillips, M. C. The charge and structural stability of apolipoprotein A-I in discoidal and spherical recombinant high density lipoprotein particles. *J. Biol. Chem.* **267**, 25839–25847 (1992).
51. Sparks, D. L., Frank, P. G. & Neville, T. A. Effect of the surface lipid composition of reconstituted LPA-I on apolipoprotein A-I structure and lecithin: cholesterol acyltransferase activity. *Biochim. Biophys. Acta* **1390**, 160–172 (1998).
52. Sparks, D. L., Davidson, W. S., Lund-Katz, S. & Phillips, M. C. Effect of cholesterol on the charge and structure of apolipoprotein A-I in recombinant high density lipoprotein particles. *J. Biol. Chem.* **268**, 23250–23257 (1993).
53. Borhani, D. W., Rogers, D. P., Engler, J. A. & Brouillette, C. G. Crystal structure of truncated human apolipoprotein A-I suggests a lipid-bound conformation. *Proc. Natl. Acad. Sci.* **94**, 12291–12296 (1997).
54. Mahley, R. W. Apolipoprotein E: cholesterol transport protein with expanding role in cell biology. *Science* **240**, 622–630 (1988).
55. Huang, Y., Weisgraber, K. H., Mucke, L. & Mahley, R. W. Apolipoprotein E: diversity of cellular origins, structural and biophysical properties, and effects in Alzheimer's disease. *J. Mol. Neurosci.* **23**, 189–204 (2004).
56. Huang, Y. & Mahley, R. W. Apolipoprotein E: structure and function in lipid metabolism, neurobiology, and Alzheimer's diseases. *Neurobiol. Dis.* **72 Pt A**, 3–12 (2014).
57. Weisgraber, K. H. Apolipoprotein E: structure-function relationships. *Adv. Protein Chem.* **45**, 249–302 (1994).
58. Innerarity, T. L., Friedlander, E. J., Rall, S. C. J., Weisgraber, K. H. & Mahley, R. W. The receptor-binding domain of human apolipoprotein E. Binding of apolipoprotein E fragments. *J. Biol. Chem.* **258**, 12341–12347 (1983).

59. Wilson, C., Wardell, M. R., Weisgraber, K. H., Mahley, R. W. & Agard, D. A. Three-dimensional structure of the LDL receptor-binding domain of human apolipoprotein E. *Science* **252**, 1817–1822 (1991).
60. Mahley, R. W. & Huang, Y. Atherogenic remnant lipoproteins: role for proteoglycans in trapping, transferring, and internalizing. *J. Clin. Invest.* **117**, 94–98 (2007).
61. Futamura, M. *et al.* Two-step mechanism of binding of apolipoprotein E to heparin: implications for the kinetics of apolipoprotein E-heparan sulfate proteoglycan complex formation on cell surfaces. *J. Biol. Chem.* **280**, 5414–5422 (2005).
62. Narita, M. *et al.* Cellular catabolism of lipid poor apolipoprotein E via cell surface LDL receptor-related protein. *J. Biochem.* **132**, 743–749 (2002).
63. Libeu, C. P. *et al.* New insights into the heparan sulfate proteoglycan-binding activity of apolipoprotein E. *J. Biol. Chem.* **276**, 39138–39144 (2001).
64. Saito, H. *et al.* Characterization of the heparin binding sites in human apolipoprotein E. *J. Biol. Chem.* **278**, 14782–14787 (2003).
65. Chen, J., Li, Q. & Wang, J. Topology of human apolipoprotein E3 uniquely regulates its diverse biological functions. *Proc. Natl. Acad. Sci. U. S. A.* **108**, 14813–14818 (2011).
66. Frieden, C., Wang, H. & Ho, C. M. W. A mechanism for lipid binding to apoE and the role of intrinsically disordered regions coupled to domain-domain interactions. *Proc. Natl. Acad. Sci. U. S. A.* **114**, 6292–6297 (2017).
67. Farrah, T. *et al.* A high-confidence human plasma proteome reference set with estimated concentrations in PeptideAtlas. *Mol. Cell. Proteomics* **10**, M110.006353 (2011).
68. Nguyen, D., Dhanasekaran, P., Phillips, M. C. & Lund-Katz, S. Molecular Mechanism of Apolipoprotein E Binding to Lipoprotein Particles. *Biochemistry* **48**, 3025–3032 (2009).
69. Chinnaraj, M. *et al.* Structure of prothrombin in the closed form reveals new details on the mechanism of activation. *Sci. Rep.* **8**, 2945 (2018).
70. Yang, A. H. *et al.* Crystal structures of two mutants (K206Q, H207E) of the N-lobe of human transferrin with increased affinity for iron. *Protein Sci.* **9**, 49–52 (2000).
71. Bhattacharya, A. A., Curry, S. & Franks, N. P. Binding of the general anesthetics propofol and halothane to human serum albumin. High resolution crystal structures. *J. Biol. Chem.* **275**, 38731–38738 (2000).
72. Lee, Y. *et al.* Glycosylation and sialylation of macrophage-derived human apolipoprotein E analyzed by SDS-PAGE and mass spectrometry: Evidence for a novel site of glycosylation on SER290. *Mol. Cell. Proteomics* **9**, 1968–1981 (2010).
73. Campbell, F. *et al.* Directing Nanoparticle Biodistribution through Evasion and Exploitation of Stab2-Dependent Nanoparticle Uptake. *ACS Nano* **12**, 2138–2150 (2018).
74. Arias-Alpizar, G. *et al.* Stabilin-1 is required for the endothelial clearance of small anionic nanoparticles. *Nanomedicine Nanotechnology, Biol. Med.* **34**, 102395 (2021).

